Interaction of Individual Skyrmions in a Nanostructured Cubic Chiral Magnet

Haifeng Du,[1,2] Xuebing Zhao,[3] Filipp N. Rybakov,[4] Aleksandr B. Borisov,[5] Shasha Wang,[1] Jin Tang,[1] Chiming Jin,[1] Chao Wang,[3] Wensheng Wei,[1] Nikolai S. Kiselev,[6,*] Yuheng Zhang,[1,7,8] Renchao Che,[3,†] Stefan Blügel,[6] and Mingliang Tian[1,2,8,‡]

[1]*The Anhui Province Key Laboratory of Condensed Matter Physics at Extreme Conditions, High Magnetic Field Laboratory, Chinese Academy of Sciences and University of Science and Technology of China, Hefei 230026, China*
[2]*Department of Physics, School of Physics and Materials Science, Anhui University, Hefei 230601, China*
[3]*Laboratory of Advanced Materials, Department of Materials Science, Collaborative Innovation Center of Chemistry for Energy Materials, Fudan University, Shanghai 200438, China*
[4]*Department of Physics, KTH-Royal Institute of Technology, Stockholm, SE-10691 Sweden*
[5]*M.N. Miheev Institute of Metal Physics of Ural Branch of Russian Academy of Sciences, Ekaterinburg 620990, Russia*
[6]*Peter Grünberg Institute and Institute for Advanced Simulation, Forschungszentrum Jülich and JARA, 52425 Jülich, Germany*
[7]*Department of Physics, University of Science and Technology of China, Hefei 230031, China*
[8]*Collaborative Innovation Center of Advanced Microstructures, Nanjing University, Nanjing 210093, China*

(Received 31 October 2017; revised manuscript received 9 March 2018; published 11 May 2018)

We report direct evidence of the field-dependent character of the interaction between individual magnetic skyrmions as well as between skyrmions and edges in $B20$-type FeGe nanostripes observed by means of high-resolution Lorentz transmission electron microscopy. It is shown that above certain critical values of an external magnetic field the character of such long-range skyrmion interactions changes from attraction to repulsion. Experimentally measured equilibrium inter-skyrmion and skyrmion-edge distances as a function of the applied magnetic field shows quantitative agreement with the results of micromagnetic simulations. The important role of demagnetizing fields and the internal symmetry of three-dimensional magnetic skyrmions are discussed in detail.

DOI: 10.1103/PhysRevLett.120.197203

Magnetic chiral skyrmions are topological solitons appearing in magnetic crystals with broken inversion symmetry [1]. The stability or metastability of such particle-like objects is provided by the competition between Heisenberg exchange, Dzyaloshinskii-Moriya interaction (DMI), and interaction with an applied field [2–7]. Their small size, topological protection, and high mobility make them hold great promise as data bit carriers in a novel type of magnetic memory and logical elements for spintronics [8–10]. For applications as well as for fundamental research, one of the key questions concerns the character of skyrmion-skyrmion and skyrmion-edge interactions, which define the equilibrium interparticle distances and place certain restrictions on the data capacity and ultimate operation speed [11–13].

Magnetic skyrmions are also known to be stable in ultrathin films and multilayers with strong perpendicular anisotropy and surface- or interface-induced DMI [14,15]. Such two-dimensional (2D) skyrmions show a long-range interparticle repulsion [5,13,16] and share a lot of similarities with magnetic bubble domains in perpendicular anisotropy films or multilayers [17,18] and the vortices in type-II superconductors [19]. The focus of this work is on the experimental and theoretical study of the inter-skyrmion and skyrmion-edge interactions in cubic chiral magnets with bulk-type DMI.

Contrary to 2D systems, in cubic chiral magnets the skyrmions are inhomogeneous along the film thickness and form three-dimensional (3D) skyrmion tubes (SkTs) with an extra twist at the ends [20] due to the effect of the chiral surface twist [21]. Moreover, in a wide range of external magnetic fields B_{ext}, the ground state corresponds to a cone phase characterized by chiral modulations of magnetization along $\mathbf{B}_{\mathrm{ext}}$ and represents a nonhomogeneous "vacuum" for 3D SkTs. Such SkTs first were investigated theoretically in Ref. [22], where it was shown that in a certain range of parameters the single SkT embedded in the metastable cone phase represents an energetically unfavorable state, while the global energy minimum corresponds to the lattice of such SkTs. This fact indicates that the clumping of 3D SkTs may lead to a significant decrease of the total energy. Later, by means of numerical methods it was established that the asymptotic behavior of a 3D SkT possesses a positive energy density with respect to the surrounding cone phase [23]. Because of that, the interparticle as well as particle-edge interactions of 3D SkTs should have the character of long-range attraction [24], which naturally leads to the formation of skyrmion pairs (dimers) and large skyrmion clusters. The observation of such clusters has been reported earlier in nanostructured $B20$-type FeGe [25,26] and extended plates of Cu_2OSeO_3 [27,28].

 © 2018 American Physical Society

Figure 1 shows the evolution of a skyrmion cluster in a FeGe nanostripe fabricated from a bulk crystal with the method described in Ref. [29]. The characterization of such samples with electron energy loss spectroscopy shows that the typical thickness variation does not exceed 3% [30]. At a low field the skyrmions preferentially assemble near the edges, and with an increasing field they migrate to the middle part of the stripe without a noticeable loss of their long-range order; compare Figs. 1(a) and 1(b). One has to note that an assumption of the presence of strong pinning centers, which, in general, can be considered as an alternative explanation for skyrmion clustering, in fact, is not supported by our observations, which clearly show a high mobility of the SkTs [Figs. 1(b) and 1(c)] under the action of a varied magnetic field even at the relatively low temperature $T \sim 100$ K. Moreover, in Supplemental Material [31], we describe another interesting phenomenon of spontaneous leaps of a single skyrmion between the two positions, indicating a high mobility of SkTs activated by elevating the temperature to 150 K. At high $B_{\mathrm{ext}} = 484$ mT, the long-range order in a skyrmion cluster is violated, while the skyrmions aggregate near the middle line of the stripe [Fig. 1(c)].

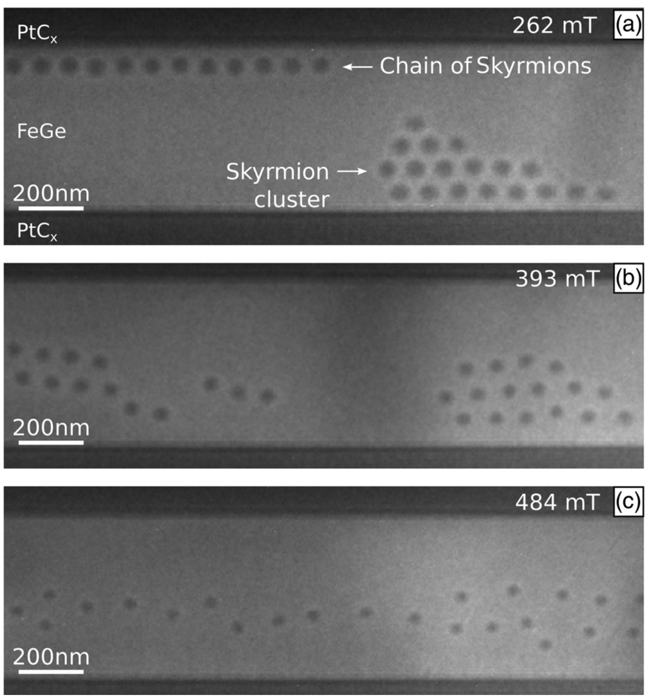

FIG. 1. Lorentz TEM images showing the evolution of skyrmion arrangement in a wide, ~500 nm, FeGe nanostripe with a thickness of ~120 nm with an increasing magnetic field applied normally to the plate. (a) A skyrmion chain and skyrmion cluster with long-range order formed near the edges of the sample at a low field. (b) A skyrmion cluster migrating to the central part of the sample with an increasing field. A long-range order in skyrmion arrangement and the distance between skyrmions is conserved. (c) A disordered skyrmion cluster in the middle part of the nanostripe at a high magnetic field. The distance between skyrmions is not conserved. All Lorentz-TEM images are taken at $T = 100$ K in underfocus conditions with a focused value of ~300 μm.

On a qualitative level, the attractive skyrmion-skyrmion interaction can be a good explanation for these observations at a low field, and the violation of the long-range order at a high field may serve as an indicator that the character of the inter-skyrmion as well as skyrmion-edge interaction changes from attraction to repulsion. Nevertheless, it is well known that even purely repulsive particles can form clusters and clumps [36,37]. Thereby, the clustering itself is not a sufficient argument in favor of the hypothesis of long-range inter-skyrmion attraction.

In order to reveal the genuine character of skyrmion interactions, one has to go beyond the collective phenomena and study the isolated skyrmion pairs. Besides that, an adequate theoretical model for skyrmion interactions must be in quantitative agreement with the experimental data, which in turn requires taking into account the effects of a stray field (dipole-dipole interaction) which is always naturally present. Such a long-range interaction is known to be significant in such systems [38] but was ignored in earlier studies on skyrmion interactions [23,24,27,28]. In the following, we present complementary experimental and theoretical results unambiguously revealing the details of the inter-skyrmion and skyrmion-edge interactions.

Figure 2 shows the field-driven evolution of two pairs of SkTs at increasing [Figs. 2(a)–2(f)] and decreasing B_{ext} [Figs. 2(g)–2(l)] in the nanostripe. We measured the field dependence of equilibrium inter-skyrmion and skyrmion-edge distances and identified the critical value of B_{ext}, above which the SkTs start to weakly repel each other. The initial state with a reduced number of SkTs [Fig. 2(a)] has been achieved via the control of the number of helical spirals in the nanostripe, which in turn can be adjusted during the demagnetization process. As has been revealed in our earlier experiments, at low temperatures, each period of the helix converges to one single SkT by increasing B_{ext} [25]. At $B_{\mathrm{ext}} = 255$ mT, two pairs of skyrmions are positioned near the edge of the sample at a large distance; thus, the interaction between pairs is negligible. Up to a magnetic field of ~400 mT, the nearest skyrmion-skyrmion distance d_{ss} remains almost unchanged [Figs. 2(a)–2(d)], but in the range from 400 to 500 mT, it increases abruptly [Figs. 2(e) and 2(f)]. In contrast to d_{ss}, the skyrmion-edge distance d_{se} increases gradually at small B_{ext} [Figs. 2(a)–2(c)] and starts to increase abruptly above 350 mT. At a higher $B_{\mathrm{ext}} \sim 500$ mT, the skyrmions are distributed in the middle of the nanostripe and show a very weak variation in their positions with a farther increasing field up to collapse. The observed behavior clearly demonstrates that the character of the inter-skyrmion interaction can be switched from strong attractive at a low field to weakly repulsive at high B_{ext}. The above-discussed behavior of skyrmions is well reproduced (a complete field-driven motion of the skyrmion is shown in

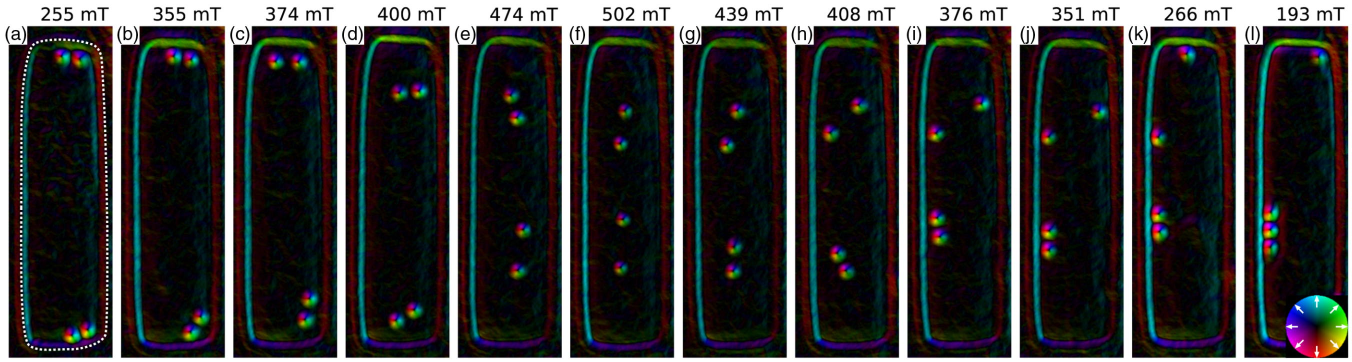

FIG. 2. Field-driven evolution of interacting pairs of skyrmions in a nearly rectangular FeGe plate [the boundaries are marked in (a) with white dotted lines] with a width, length, and thickness of 430, 1590, and 120 nm, respectively. Color represents the direction of the in-plane component of magnetization; see the inset in (l). Attractive skyrmion-skyrmion and skyrmion-edge interactions are observed at a low magnetic field, while at a high magnetic field the character of the interactions changes to repulsive. Increasing (a)–(f) and decreasing (g)–(l) field magnetization processes illustrate the reversibility of the states with a very weak hysteresis effect. The lower-left isolated skyrmion and corresponding skyrmion pair are chosen to estimate the inter-skyrmion and skyrmion-edge distances, respectively, with the data presented in Figs. 3(c) and 3(d).

Supplemental Video 2 [31]) and is almost unchanged when the sample is tilted with respect to the plane normal up to 5° [31].

An important feature of the field-driven evolution of inter-skyrmion and skyrmion-edge distances is its full reversibility. Otherwise, a possible explanation would be the presence of the pinning centers which obstruct skyrmions from running away from one another. With decreasing B_{ext} down to 408 mT [Fig. 2(h)], the d_{ss} of the bottom pair is significantly decreased, which indicates the appearance of an attractive interaction again. It is seen that the top pair of particles has been severed due to the attraction acting on each skyrmion from the side of the opposite edges of the sample. With a further decreasing of the field, all SkTs move close to the edge and either form a paired state or remain isolated [Figs. 2(i)–2(k)]. It is worth paying attention to the relatively large distance between a single SkT and a pair of SkTs on the left side of the sample at 266 mT [Fig. 2(k)]. Despite the extremely large distance between them, these three skyrmions form a chain when B_{ext} further reduces down to 193 mT [Fig. 2(l)], suggesting that SkTs are able to attract each other at distances much larger than the characteristic size of the skyrmions, L_D.

This attractive interaction can be well understood in the following way. At a low magnetic field, the isolated skyrmion is surrounded by the cone phase, giving rise to a nontrivial 3D SkT [Fig. 3(a)]. When two such inhomogeneous SkTs approach each other, the mutual volume of the pair turns out to be smaller than the total volume of two isolated SkTs [Fig. 3(b)]. Accordingly, the total energy of such a coupled state with respect to the energy of the cone phase becomes lower and makes the coupled SkTs energetically more favorable than two isolated SkTs. However, too small a distance between two SkTs leads to an additional distortion of the spin configuration of the two SkTs, which are energetically unfavorable. The competitions of these two effects, (i) reduction of the total volume occupied by the coupled two SkTs and (ii) distortion of isolated SkTs, results in an equilibrium inter-skyrmion distance with a Lennard-Jones–like potential of interparticle interaction [23]. Moreover, a strict mathematical analysis of the basic model of the isotropic chiral magnet revealed that the spin texture of an isolated SkT appearing as an excitation on the background of the conical phase has hidden symmetry. The latter means that, without any loss of generality, the exact solution for an isolated translationally invariant SkT, as shown in Fig. 3(a), can be obtained via a special 2D model Hamiltonian; for details, see Ref. [31]. This solution corresponds to a 2D "oblique" skyrmion (similar to the texture of the pair of half lumps in the easy plane baby Skyrme model [39] and skyrmions in a tilted magnetic field [40,41]), as shown in Fig. 3(c), in a ferromagnetic background inclined by angle θ_{cone} with respect to $\mathbf{B}_{\mathrm{ext}}$ corresponding to an equilibrium angle of the conical phase. The complete spin texture of 3D SkT is then followed from analytical mapping based on an affine transformation. Although in films of finite thickness the additional twists of magnetization arise near the surfaces [20], the underlying part of the tube preserves the aforementioned symmetry. The presence of another SkT in the system in turn breaks this symmetry, as well illustrated by means of overlapping isosurfaces of two SkTs in Figs. 3(b) and 3(d). The line which connects the cores cannot be preserved under the affine transformation. Coupled SkTs can be considered as one object which is also a skyrmionic solution with a higher topological charge.

To validate experimentally observed behaviors, we performed micromagnetic simulations by means of MuMax^3 [42] for a realistic specimen geometry [31]. The theoretical curves in Figs. 3(e) and 3(f) are in very good qualitative and quantitative agreement with the experimental data. For the critical fields $B_{\mathrm{se}} \sim 420$ mT

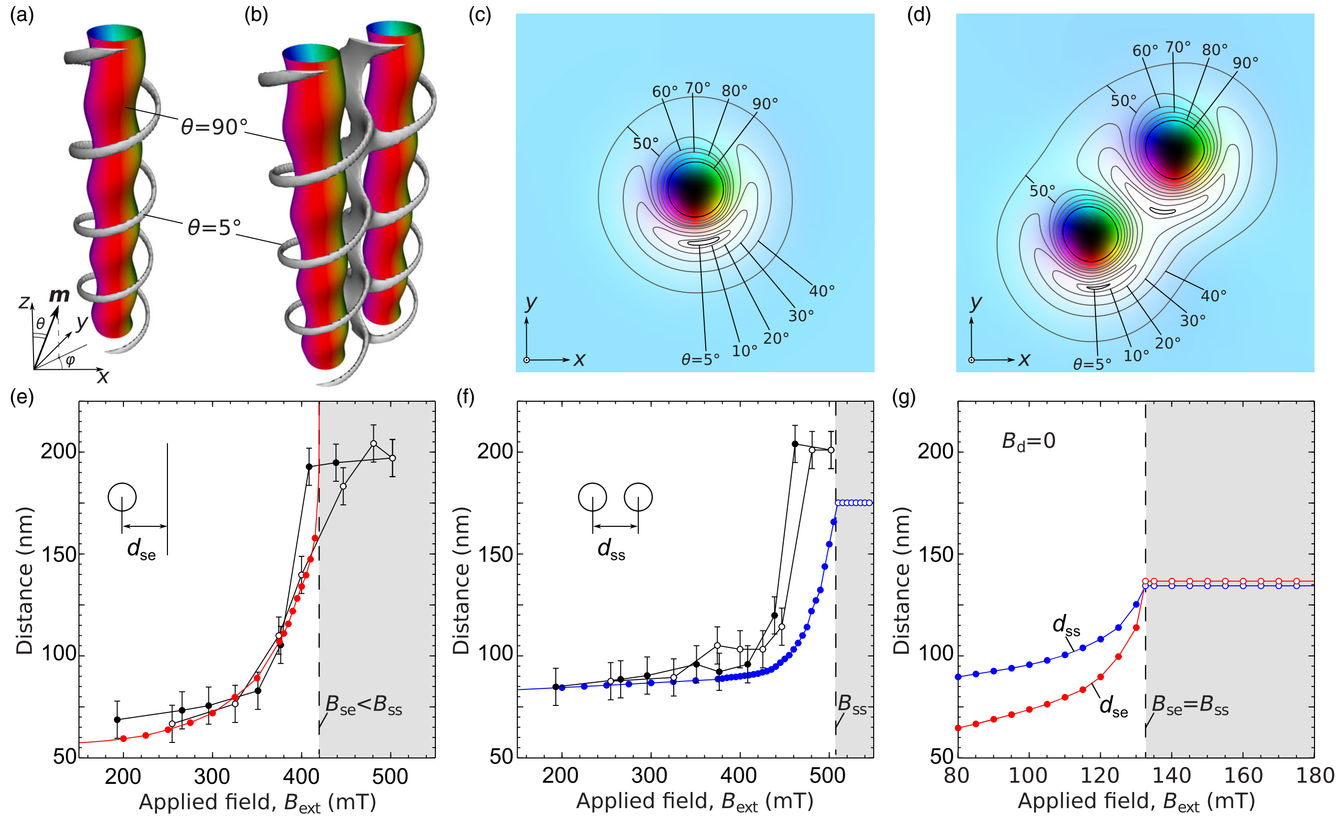

FIG. 3. (a) and (b) represent the isosurfaces $\theta = 90°$ and $\theta = 5°$ for a typical segment of a single SkT and a coupled pair of SkTs, respectively, while for a finite thickness film the corresponding SkTs are characterized by distortion near the ends of the tube due to the chiral surface twist [20]. The standard color code indicates the direction of the magnetic moments on a unit sphere, where black and white correspond to $m_z = -1$ ($\theta = 180°$) and $m_z = +1$ ($\theta = 0°$), respectively. (c) and (d) represent a cross section of a SkT and a pair of SkTs shown in (a) and (b) with $z = \text{const}$ plane. Closed curves indicate isolines for the θ angle. (e) Skyrmion-edge distance as a function of the field. (f) Skyrmion-skyrmion distance. Open and solid (black) circles in (c) and (d) correspond to an increasing and a decreasing field, respectively. Red and blue circles represent theoretical dependencies. (g) The theoretical dependencies for d_{se} and d_{ss} calculated in the assumption of a demagnetizing field inside the sample, $B_d = 0$.

and $B_{ss} \sim 510$ mT, the corresponding theoretical dependencies for d_{se} and d_{ss} tend to infinity, which reflects the change in the character of interactions from attractive to repulsive. It happens because at strong B_{ext} the cone phase reaches saturation, which means that the "vacuum" surrounding SkTs become field polarized and isotropic. The SkTs in such a ferromagnetic background possessing a radially symmetric structure behave identically to skyrmions in a 2D system and always repel each other [5]. Thereby, the measured value of critical field B_{ss} also can be thought as the saturation field for the conical phase.

It is important to note the difference between the values of critical fields B_{se} and B_{ss}. As follows from experimental and theoretical dependencies presented in Figs. 3(e) and 3(f), $B_{se} < B_{ss}$, meaning that the skyrmion-edge interaction changes its character to repulsive at a significantly lower field compare to the inter-skyrmion interaction. For $B_{se} < B_{ext} < B_{ss}$, SkTs form clusters far from the edges in the center of the sample. This agrees with the recently observed effect of skyrmion clustering in the center of a FeGe plate [43]. In order to reveal the nature of this effect, we performed a comparative calculation for d_{se} and d_{ss}, where we ignore the energy contribution of the demagnetizing field [Fig. 3(g)]. Besides the significant reduction of the absolute values of B_{se} and B_{ss}, which reflect the important role of demagnetizing fields for quantitative agreement, one can clearly see that the dependencies for d_{se} and d_{ss} tend to infinity at the same critical field, $B_{se} = B_{ss}$. The latter means that the effect of skyrmion clustering in the center of the sample reflects the strong influence of demagnetizing fields. Both d_{se} and d_{ss} exhibit a nearly constant value above the critical field. Such saturation occurs because the energy contribution of weak inhomogeneities, thermal fluctuations, etc., becomes comparable to or even exceeds the repulsive inter-skyrmion forces which are exponentially small at large distances. In the simulations, the saturation of d_{se} and d_{ss} is mainly caused by the finite precision of the numerical calculations. All the aforementioned effects are also observed in large size samples and can be well explained in terms of forces of inter-skyrmion and skyrmion-edge interactions and their dependences on an external magnetic field provided in Supplemental Material [31].

In summary, we present the first experimental evidence for a Lennard-Jones–type interaction between individual skyrmions revealed by the direct observation of the reversible field-driven evolution of interparticle equilibrium distances. In good agreement with the results of micromagnetic simulations, it is shown that with an increasing field the character of long-range skyrmion interactions changes from attractive to repulsive. Finally, it is worth emphasizing that the revealed mechanism of attractive interaction for 3D skyrmions is completely different from other systems such as, for instance, frustrated 2D magnets [44] or type-1.5 superconductors [45].

This work was supported by the National Key R&D Program of China, Grant No. 2017YFA0303201, the Key Research Program of Frontier Sciences, CAS, Grant No. QYZDB-SSW-SLH009, the Natural Science Foundation of China, Grants No. 51622105 and No. 11474290, the Key Research Program of the Chinese Academy of Sciences, KJZD-SW-M01, the Major/Innovative Program of Development Foundation of Hefei Center for Physical Science and Technology, Grant No. 2016FXCX001, and the Youth Innovation Promotion Association CAS No. 2015267. The work of F. N. R. was supported by the Swedish Research Council Grant No. 642-2013-7837 and by Göran Gustafsson Foundation for Research in Natural Sciences and Medicine. The research of A. B. B. was carried out within the state assignment of FASO of Russia (theme "Quantum" No. 01201463332). The authors would like to thank E. Babaev for helpful discussions.

*n.kiselev@fz-juelich.de
†rcche@fudan.edu.cn
‡tianml@hmfl.ac.cn

[1] A. N. Bogdanov and D. A. Yablonskii, Sov. Phys. JETP **68**, 101 (1989).
[2] B. A. Ivanov, V. A. Stephanovich, and A. A. Zhmudskii, J. Magn. Magn. Mater. **88**, 116 (1990).
[3] I. Dzyaloshinskii, J. Phys. Chem. Solids **4**, 241 (1958).
[4] T. Moriya, Phys. Rev. **120**, 91 (1960).
[5] A. Bogdanov, Pis'ma Zh. Eksp. Teor. Fiz. **62**, 231 (1995) [JETP Lett. **62**, 247 (1995)].
[6] X. Z. Yu, Y. Onose, N. Kanazawa, J. H. Park, J. H. Han, Y. Matsui, N. Nagaosa, and Y. Tokura, Nature (London) **465**, 901 (2010).
[7] N. Nagaosa and Y. Tokura, Nat. Nanotechnol. **8**, 899 (2013).
[8] N. S. Kiselev, A. N. Bogdanov, R. Schäfer, and U. K. Rößler, J. Phys. D **44**, 392001 (2011).
[9] A. Fert, V. Cros, and J. Sampaio, Nat. Nanotechnol. **8**, 152 (2013).
[10] X. Zhang, M. Ezawa, and Y. Zhou, Sci. Rep. **5**, 9400 (2015).
[11] J. Iwasaki, M. Mochizuki, and N. Nagaosa, Nat. Nanotechnol. **8**, 742 (2013).
[12] J. Sampaio, V. Cros, S. Rohart, A. Thiaville, and A. Fert, Nat. Nanotechnol. **8**, 839 (2013).
[13] X. Zhang, G. P. Zhao, H. Fangohr, J. P. Liu, W. X. Xia, J. Xia, and F. J. Morvan, Sci. Rep. **5**, 7643 (2015).
[14] N. Romming, A. Kubetzka, C. Hanneken, K. von Bergmann, and R. Wiesendanger, Phys. Rev. Lett. **114**, 177203 (2015).
[15] O. Boulle *et al.*, Nat. Nanotechnol. **11**, 449 (2016).
[16] U. K. Rößler, A. A. Leonov, and A. N. Bogdanov, J. Phys. Conf. Ser. **303**, 012105 (2011).
[17] A. H. Bobeck and E. Della Torre, *Magnetic Domain Walls in Bubble Materials* (North-Holland, Amsterdam, 1979).
[18] A. Hubert and R. Schäfer, *Magnetic Domains* (Springer-Verlag, Berlin, 1998).
[19] G. Stan, S. B. Field, and J. M. Martinis, Phys. Rev. Lett. **92**, 097003 (2004).
[20] F. N. Rybakov, A. B. Borisov, and A. N. Bogdanov, Phys. Rev. B **87**, 094424 (2013).
[21] S. A. Meynell, M. N. Wilson, H. Fritzsche, A. N. Bogdanov, and T. L. Monchesky, Phys. Rev. B **90**, 014406 (2014).
[22] F. N. Rybakov, A. B. Borisov, S. Blügel, and N. S. Kiselev, Phys. Rev. Lett. **115**, 117201 (2015).
[23] A. O. Leonov, T. L. Monchesky, J. C. Loudon, and A. N. Bogdanov, J. Phys. Condens. Matter **28**, 35LT01 (2016).
[24] A. O. Leonov, J. C. Loudon, and A. N. Bogdanov, Appl. Phys. Lett. **109**, 172404 (2016).
[25] H. Du, R. Che, L. Kong, X. Zhao, C. Jin, C. Wang, J. Yang, W. Ning, R. Li, C. Jin, X. Chen, J. Zang, Y. Zhang, and M. Tian, Nat. Commun. **6**, 8504 (2015).
[26] X. Zhao, C. Jin, L. Kong, C. Wang, H. Du, J. Zang, M. Tian, R. Che, and Y. Zhang, Proc. Natl. Acad. Sci. U.S.A. **113**, 4918 (2016).
[27] J. Müller, J. Rajeswari, P. Huang, Y. Murooka, H. M. Ronnow, F. Carbone, and A. Rosch, Phys. Rev. Lett. **119**, 137201 (2017).
[28] J. C. Loudon, A. O. Leonov, A. N. Bogdanov, M. Ciomaga Hatnean, and G. Balakrishnan, Phys. Rev. B **97**, 134403 (2018).
[29] C. Jin, Z.-A. Li, A. Kovács, J. Caron, F. Zheng, F. N. Rybakov, N. S. Kiselev, H. Du, S. Blügel, M. Tian, Y. Zhang, M. Farle, and R. E. Dunin-Borkowski, Nat. Commun. **8**, 15569 (2017).
[30] C. Wang, H. Du, X. Zhao, C. Jin, M. Tian, Y. Zhang, and R. Che, Nano Lett. **17**, 2921 (2017).
[31] See Supplemental Material at http://link.aps.org/supplemental/10.1103/PhysRevLett.120.197203 for two video files, the description of the phenomenon of a spontaneous leap of a single skyrmion between two metastable positions, a discussion of the reproducibility of the experimental data, the effect of an inclined field, basic model analyses, details of micromagnetic simulations, and an estimation of conservative forces, which includes Refs. [32–35].
[32] V. G. Bar'yakhtar and E. P. Stefanovsky, Fiz. Tverd. Tela **11**, 1946 (1969); Sov. Phys. Solid State **11**, 1566 (1970).
[33] P. Bak and M. H. Jensen, J. Phys. C **13**, L881 (1980).
[34] M. Beg, R. Carey, W. Wang, D. Cortés-Ortuño, M. Vousden, M.-A. Bisotti, M. Albert, D. Chernyshenko, O. Hovorka, R. L. Stamps, and H. Fangohr, Sci. Rep. **5**, 17137 (2015).
[35] I. E. Dzyaloshinskii, Sov. Phys. JETP **20**, 665 (1965).

[36] W. Klein, H. Gould, R. A. Ramos, I. Clejan, and A. I. Mel'cuk, Physica (Amsterdam) **205A**, 738 (1994).
[37] M. A. Glaser, G. M. Grason, R. D. Kamien, A. Kosmrlj, C. D. Santangelo, and P. Ziherl, Europhys. Lett. **78**, 46004 (2007).
[38] K. Shibata, A. Kovács, N. S. Kiselev, N. Kanazawa, R. E. Dunin-Borkowski, and Y. Tokura, Phys. Rev. Lett. **118**, 087202 (2017).
[39] J. Jäykkä and M. Speight, Phys. Rev. D **82**, 125030 (2010).
[40] S.-Z. Lin and A. Saxena, Phys. Rev. B **92**, 180401(R) (2015).
[41] A. O. Leonov and I. Kézsmárki, Phys. Rev. B **96**, 214413 (2017).
[42] A. Vansteenkiste, J. Leliaert, M. Dvornik, M. Helsen, F. Garcia-Sanchez, and B. Van Waeyenberge, AIP Adv. **4**, 107133 (2014).
[43] F. Zheng, F. N. Rybakov, A. B. Borisov, D. Song, S. Wang, Z.-A. Li, H. Du, N. S. Kiselev, J. Caron, A. Kovács, M. Tian, Y. Zhang, S. Blügel, and R. E. Dunin-Borkowski, Nat. Nanotechnol., DOI: 10.1038/s41565-018-0093-3 (2018).
[44] L. Rózsa, A. Deák, E. Simon, R. Yanes, L. Udvardi, L. Szunyogh, and U. Nowak, Phys. Rev. Lett. **117**, 157205 (2016).
[45] E. Babaev and M. Speight, Phys. Rev. B **72**, 180502(R) (2005).